Published paper
Yan, Y., Neville, A. and Dowson, D. (2007) *Tribo-corrosion properties of cobalt-based medical implant alloys in simulated biological environments,* Wear, Volume 263 (7-12), 1417 - 1422.

Tribo-corrosion properties of Cobalt-based medical implant alloys in simulated biological environments

Yu Yan*, Anne Neville and Duncan Dowson
School of Mechanical Engineering, University of Leeds, Leeds, LS2 9JT, UK
*Tel: 0044 (0) 1133432179
Fax: 0044 (0) 1132424611
E mail: menyya@leeds.ac.uk

Abstract

Tribological problems and corrosion degradation have been recognized as essential risks for total joint replacements, especially for all-metal arthroplasty. Few studies have focused on the interactions between tribology and corrosion (tribocorrosion) for implant materials. This paper addresses the importance of understanding tribocorrosion and the evaluation of such materials in simulated biological environments. Due to the complex effect of proteins on tribocorrosion, which has been demonstrated in previous studies, this study focuses towards understanding the effects of amino acids as aspects of material degradation. Dulbecco's Modified Eagle's Medium (DMEM) is a cell culture solution. It contains comparable amount and types of amino acids to normal synovial fluid in human joints. 0.36% NaCl solution was employed to isolate the biological species. Three materials were tested; High carbon (HC) CoCrMo (contains 0.19% carbon), low carbon (LC) CoCrMo (widely used materials for total joint replacement) and stainless steel UNS S31603 (316L). Integrated electrochemical tests supported by measurement of friction and near surface chemical analysis were carried out to enable their tribocorrosion behaviour to be fully characterized. As a general conclusion, amino acids were found to react with materials under tribological contacts and form complex organometallic/oxides which lubricate the metallic sample surface. Tribocorrosion plays a very important role in material degradation in the studied environments. HC CoCrMo shows superior wear, corrosion and tribocorrosion resistance – the material characteristics and their effect on the different tribocorrosion

processes are discussed.

Keywords

Wear; Corrosion; Implant; Cobalt alloys; Electrochemical tests; Friction.

Introduction

A renewed interest in Metal-on-Metal (MoM) prosthesis bearings has been considered and developed since the early 1990s [1-3]. This has been mainly due to the problems of polyethylene wear debris induced osteolysis from the widely used Polyethylene-on-Metal (PoM) total joint arthroplasty [4]. However, MoM joint replacements are not used by surgeons without concerns, released metal ions from MoM pairs may cause cytotoxicity, tissue necrosis, adverse immunological reactions and hypersensitivity [5, 6]. Therefore, it is rather urgent and important to have a better understanding of the metal ion release processes for metallic orthopaedic implant materials.

Metal ion release is an electrochemical process; generally denoted as corrosion. There is a general agreement that corrosion is a serious problem for medical metallic materials [7, 8]. For joint replacements, they perform under tribological contacts and load. Their performance (long-term durability) relies on both of their corrosion resistance and wear resistance. Many studies have been carried out world wide for either tribology behavior or corrosion behavior of joint replacement materials and components [9-11]. However, research of the synergistic effect of corrosion and tribology still lacks for this application. Corrosion accelerates the wear rate and vice versa in many industries. This study therefore focuses on the role of corrosion in this system (tribo-corrosion system) and the interactions of corrosion and tribology in the simulated biological environments.

Cobalt-based alloys have been widely used in implant components, especially in orthopaedic implants due to their high corrosion resistance and wear properties. Two types of Cobalt-based alloys are the most popular implant materials. They both have balanced Cobalt content with approximately 28% Chromium and 5% Molybdenum. The difference between them is that one has a higher carbon content (0.15-0.25%); the other has a lower carbon content (less then 0.06%) [12]. Much progress has been made in Cobalt-based metallic implants development to reduce total volumetric wear. Much of this has been focused towards design and in particular using a larger diameter of femoral head, better surface finish, a thinner acetabular cup and a smaller clearance (50-90 μm) between the acetabular cup and the femoral head [13, 14].

However, the joint replacement operates in biological environment (corrosive). The influence of the biological species is also of great important. Studies have been carried out by the current authors and other research groups to understand the effect of proteins in synovial fluids on the tribological and corrosion properties of implant materials [15-21]. The effect of proteins on tribocorrosion is complicated and depends on the types of protein and tested materials. The denatured proteins play an important role in the formation of the tribofilm as demonstrated in [19]. Therefore in this study, how amino acids affect the tribocorrosion behaviour of Co-based alloys is one of the main focuses.

Materials and Experiment Methods

Integrated electrochemical tests were performed using a ball-on-plate reciprocating tribo-tester. Silicon nitride ball (12 mm in diameter) was chosen as the counterpart. A three-electrode cell was employed, which a standard and common method to evaluate the corrosion behaviour. A schematic representation

of the tribocorrosion cell is shown in Figure 1. The three electrodes are the working electrode (specimen), the reference electrode (Ag/AgCl electrode) and the counter electrode (Platinum). The sliding wear tests, which conformed to ASTM G133, were performed with the three-electrode cell. The applied load of 80N was chosen and the frequency of the sliding was controlled at 1Hz.

Dulbecco's Modified Eagle's Medium (DMEM) and 0.36% NaCl were used as the lubricant solutions to enable the effect of amino acids in wear-corrosion to be isolated. The conductivity of both solutions was controlled at 0.68mS/cm, which is comparable to synovial fluid. Wrought High Carbon Cobalt-Chromium-Molybdenum alloy (HC CoCrMo) and Low Carbon Cobalt-Chromium-Molybdenum alloy (LC CoCrMo) are commonly used MoM components materials and were tested with a reference stainless steel UNS S31603 (316L). The chemical composition of the three materials and their micro hardness values are shown in Table 1.

The electrochemical analysis consisted of four types of tests are described below:

1. Free corrosion potential (E_{corr}) measurements

In an electrolyte, the potential that the material adopts when it is not connected to any external electrical source is called the free corrosion potential (E_{corr}). At E_{corr} the anodic reaction rate is equal to the cathodic reaction rate. The E_{corr} can give a semi-quantitative assessment of the corrosion regime in which the material resides. In this paper, materials were exposed to tribological contact; the passive film of the tested specimens was removed and re-built. E_{corr} measurement can give a clear indication of this process [20].

2. Cathodic protection

Cathodic protection (CP) by the impressed current method is a technique to prevent corrosion. It has been broadly used in many industries. The technique was used here to isolate the pure mechanical damage and corrosion-related damage. Under CP, the reaction of Co to Co^{2+} was essentially prevented. Thus, the materials were immune to corrosion and the measured damage is entirely due to mechanical effects.

3. Anodic polarization scan

This method was used to monitor the extent of passivity of the material surface and the rate of metal dissolution from the anodic reaction. The potential of the working electrode was shifted from E_{corr} in the positive direction at a rate of 15mV/min. In the passive regime, the current stays very low (less then 10 $\mu A/cm^2$) due to the protection of the film to the charge transfer. After the potential reaches a breakdown potential (E_b), the current then will increase rapidly. This method can evaluated the effect of tribological contacts on materials corrosion behaviour.

4. Potentiostatic tests

In tribocorrosion tests, the passive film was removed by the sliding movement [19, 20]. By applying a positive potential (in the passive regime from anodic polarization scan), the mechanical depassivation and electrochemical repassivation can be monitored. In this study a potential of 0.2V was chosen.

Results and discussion

1. E_{corr} measurement

For all materials in this study, a passive film spontaneously forms in the air, protecting metal ions from being released into the bulk solution. Under sliding contact, the barrier was repeatedly removed and then re-established. By monitoring E_{corr} in conjunction with the friction force, the process can be examined. Figure 2 shows the friction coefficient and E_{corr} values for HC CoCrMo in DMEM. Before the load was applied on the specimen at point 1, the material was immersed in the solution to build a stable passive film. A clear shift in the active direction can be observed as soon as the load was added. After 4 hours rubbing, the load was removed at point 2, and the wear scar was allowed to "recover" as shown by the positive shift of potential. A transition period of potential rise was found in the initial stage of the sliding, which was due to the initial impact of mechanical movements on the passive film and the formation of a semi-passive layer of organometallic/oxides. The potential reached a relatively stable region after the transition period when an equilibrium was attained between the mechanical depassivation rate and electrochemical repassivation rate.

Comparing HC CoCrMo and LC CoCrMo in DMEM, both materials appeared to have very similar behaviour in terms of the friction coefficient and the E_{corr} values and trend (Figure 2 and Figure 3). In contrast on 316L, the potential moved to the active (negative) direction continuously until the load was removed (Figure 4). Figures 5 to 7 show the E_{corr} values and friction coefficients for HC CoCrMo, LC CoCrMo and 316L in 0.36% NaCl.

Some observations on the E_{corr}-friction coefficient correlations are made below.

- In 0.36% NaCl, all three materials showed significantly higher friction coefficient values than in DMEM, suggesting that DMEM can lubricate the sample surface by two possible mechanisms. i)

the direct lubrication from the liquid (viscosity=0.005 Pa s for DMEM and 0.001 Pa s for 0.36% NaCl); ii) an amino acid-metal complex formed and acted as a solid lubricant (tribofilm).

- Oscillations of friction and potential can be observed in DMEM and in NaCl solution. However, both friction coefficient and E_{corr} trends were smoother in 0.36% NaCl solution.
- For both Co-based alloys in DMEM, friction coefficient decreased as the E_{corr} ennobled in the initial transition period. When the potential reached a stable value, the friction coefficients had corresponding stable values.
- In 0.36% NaCl, the friction coefficient increased until it reached a stable value for all materials.

2. Material degradation

As shown in previous studies, corrosion can play a very important role in the material degradation in biotribocorrosion systems [20, 21]. The material loss under CP was measured in both DMEM and 0.36% NaCl. As shown in Figure 8, for both CoCrMo alloys in DMEM, the material loss was lower, whereas for 316L in DMEM, a slightly higher material loss was measured. XPS tests were then conducted to look at the surface properties and the formation of the tribological reaction film.

The difference of the material loss with andwithout application of CP gives the corrosion-related damage [22, 20]. Although the total material degradation in DMEM was less than in 0.36% NaCl, the proportion of corrosion was greater. Around 48% volume loss for CoCrMo alloys and 39% for 316L was attributed to corrosion-induced damage. This confirms that in such an environment the interactions of corrosion and wear, and especially the effect of corrosion on wear, have a great influence on the material degradation processes.

3. Surface analysis

The Co $2p_{3/2}$ spectra from surfaces in DMEM and 0.36% NaCl are shown in Figure 9 for HC CoCrMo. A lower amount of $Co(OH)_2$ (781.6 eV) and more Co_2O_3/CoO (779.6 eV) and organometallic formations (781.1 eV and 783.5 eV) were found in DMEM. The formation of oxides (including Cr oxides) and organometallic forms are believed to be responsible for the reduction of the friction and the lower wear rate in DMEM comparing with the same parameters in 0.36% NaCl solution. On LC CoCrMo, sulphur was observed as a sulphide form at a binding energy of 162.0 eV which corresponds to a possible CoS_2 ($Co2p_{3/2}$ at 778.4 eV). Calcium phosphate and sulphide were obtained on 316L in DMEM as well. An Fe-rich organometallic formation was obtained on 316L, which is different from the Co-rich formation on CoCrMo alloys. For CoCrMo alloys, the formations of organometallic Co and Cr with amino acids and oxides in DMEM are responsible for the reduction of the fiction (Figure 2 to Figure 7) and the reduction of wear (Figure 8). For 316L, the formations of calcium phosphate and iron sulphide enhanced the material degradation under tribological contacts, primarily due to its structure and possibility of the prevention of an important fluid film [23]. The results are consistent with previous findings in a protein-rich environment [19].

XPS tests were also carried out for samples after the application of CP. For CoCrMo alloys in 0.36% NaCl, after 5 minutes argon-ion etching, the substrate was obtained on samples without CP. It indicates that the passive film was about 15-20 nm thick. With the application of CP, the passive film was removed by 1 min argon-ion etching. It gives an indication that under CP, a thinner passive film was present than without the application of CP. In terms of the components of the passive film, there was no difference found with or without CP. The passive film contained major Cr_2O_3/CoO and $Co(OH)_2$.

In DMEM, under CP no organometallic formation was observed which indicates that corrosion (ion release process) was prevented. The adsorbed amino acid film on the passive film was thinner (5-6 nm) under CP than without the application of CP for CoCrMo. For 316L, the film thickness was about 3-4 nm with CP.

4. Linking tribological and electrochemical response

Figure 10 shows the anodic polarization curves for HC CoCrMo in DMEM and 0.36% NaCl both under rubbing and in static conditions. Three distinct regions can be identified according to the current response as shown in Figure 10. All materials showed passive behaviour in both environments in static conditions. When the sliding was conducted, in NaCl solution, the metal ions release dramatically accelerated. Even though, the current remained stable (but high) in a short potential region (between 0.3V and 0.6V); the value of the current was much greater than the same region in static conditions. In DMEM, the current initially increased (region 1) followed by a rapidly reduction of current; the stable value of current was very close to the current value in static conditions (region 2). This indicates that a passive-like barrier had formed to prevent ion release. This film contained metal oxides and organometallic formations which confirmed by XPS tests. The pseudo-passive film broke down in region 3 and the current increased again. This would be due to pitting corrosion from both inside and outside the wear scar.

The link of the tribological response (friction) to the anodic polarization scan is shown in Figure 11. The anodic polarization scans for 316L in two environments seemed to be similar, but the friction

coefficients were contrasting. In NaCl solution, a higher friction coefficient was observed than in DMEM in all three regions. However, from region 1 to region 2 in both solutions, the friction coefficient increased accordingly. It appeared that the passive film (Cr-rich oxides) in NaCl and the organometallic films in DMEM both can increase the friction for 316L. It is consistent with E_{corr} results. For CoCrMo alloys, in region 2, a reduction in friction coefficient was observed which indicates that the pseudo-passive film lubricated the sample surface.

5. Potentiostatic tests

Potentiostatic tests were carried out at a positive potential of 0.2V, chosen to be in the pseudo-passive regime during sliding according to Figure 10. The removal of the passive film and the recovery of the film can be evaluated by applying this potential and closely following the charge transfer rate. Figure 12 shows the variation in current over 2 seconds (2 cycles of reciprocating movement) with the sliding velocity. A Clear film breakdown by the rubbing action and repassivation by the electrochemical process was seen with the following observations

- The current increased in line with an increase of velocity and the current decreased with the decrease in velocity, which indicates that repassivation had taken place after the passive film was rubbed off.
- The friction force was generally uniform as a function of sliding velocity. However, as the velocity and the current increased, the friction force slightly increased. This is likely to indicate that there is some interference of hydrodynamic lubricant across the stroke length.

Tests were then carried out for 4 hours in DMEM and 0.36% NaCl at potential of 0.2V. Interestingly at around 7000 s for HC CoCrMo and 4000 s for LC CoCrMo and 316L (Figure 13 (a)(b)), a rapid reduction of current with the corresponding decrease of the friction coefficient was observed in DMEM. However, for HC CoCrMo, the reduction of current was obtained around 4000s. In these potentiostatic tests, ions were forced to be released from the material surface (mainly Co^{2+} for CoCrMo and Fe^{3+} for 316L). When the charge attained a certain value (0.39 C/cm^2 for LC CoCrMo and 0.51 C/cm^2 for 316L), a protective barrier formed to prevent any further ion release and lubricate the surface. This is entirely consistent with the anodic polarization scan results presented in the previous section and confirms the intricate relationship between the ion releases, the tribofilm formation and the friction reduction. No such reduction of current and friction can be observed in 0.36% NaCl. It gives an indication that this phenomenon is due to the reactions of amino acids with metal or metal ions in DMEM. However in 0.36% NaCl (Figure 14), the current generally increased continuously by rubbing. Only the passive film of the material was removed and re-built. This confirms that amino acids can influence the passive film formation and then influence materials tribological behaviour.

For CoCrMo alloys, in both solutions, after the potential (0.2V) was removed, the friction coefficient increased. In contrast, for 316L, a decrease of friction coefficient was observed after the potentiostatic tests stopped. It indicates that the film forced to form on CoCrMo as a result of enhanced ion release and amino acid interaction had a significant effect on lubrication. For 316L, the enhanced ion release increased the friction.

Conclusions

The understanding of the tribocorrosion behaviour of HC CoCrMo, LC CoCrMo and 316L in DMEM and 0.36% NaCl has been made based on the integrated tribo-electrochemical tests. By analyzing the tribological parameters (friction, wear, etc.) with electrochemical responses and also with chemical status of sample surfaces from XPS tests, material degradation mechanisms and the interactions between tribology, corrosion and amino acids have been discussed. The following conclusions can be obtained:

- HC CoCrMo showed the best performance in terms of high tribocorrosion resistance, low friction and low wear due to its high corrosion and wear resistance. It had about half of the material loss of LC CoCrMo and one third of 316L in tested conditions. However, the effect of released ions on the biological environment is still under investigation.
- Amino acids in DMEM lubricate the contacting materials and bind with metal or metal ions. In terms of tribofilm formation on CoCrMo alloys, in saline solution, the major components were Cr oxides and Co oxides/hydroxides. In DMEM, a thin (2-3nm) organometallic films played an important role to reduce friction and wear.
- By bringing the materials to be more electrochemically active, after an initial increase of current, a reduction of metal ion release and friction was obtained due to the organometallic formation.

References

[1] H.C. Amstutz, P. Campbell, H. McKellop, T.P. Schmalzried, W.J. Gillespie, D. Howie, J. Jacobs, J.

Medley, Metal on metal total hip replacement workshop consensus document, Clinical Orthopaedics and Related Research 319S (1996) 297-303

[2] F.W. Chan, J.D. Bobyn, J.B. Medley, J.J. Krygier, S. Yue, M. Tanzer, Engineering issues and wear performance of metal on metal hip implants, Clinical Orthopaedics and Related Research 333 (1996) 96-107

[3] H.G. Willert, G.H. Buchhorn, D. Gobel, Wear behaviour and histopathology of classic cemented metal-on-metal hip prostheses, Clinical Orthopaedics and Related Research 329 (1996) 160-186

[4] J.L. Tipper, J.B Matthews, E. Ingham, T.D Stewart, J. Fisher, Friction, Lubrication and Wear of Artificial Joints, Profession Engineering Publishing, London , pp56-78, 2003

[5] J.J. Jacobs, A.K Skipor, L.M. Patterson, N.J Hallab, W.G. Paprosky, J. Black, J.O. Galante, Metal release in patients who have had a primary total hip arthroplasty. A prospective, controlled, longitudinal study, The Journal of Bone and Joint Surgery 80 (1998) 1447-1458

[6] T. Visuri, M. Koskenvuo, Cancer risk after McKee total hip replacement, Orthopedics 14 (1991) 137-142

[7] T. Hanawa, Corrosion Measurements of Biomedical Metallic Materials, Corrosion Engineering 49 (2000) 687-699

[8] D.F. Williams, Corrosion of implant materials, Annual Review of Materials Science 6 (1976) 237-266

[9] J. Beddoes, K. Bucci, The influence of surface condition on the localized corrosion of 316L stainless steel orthopaedic implants, Journal of Materials Science: Materials In Medicine 10 (1999) 389-394

[10] M.A. Khan, R.L. Williams, D.F. Williams, The corrosion behaviour of Ti-6A1-4V,Ti-6A1-7Nb and

Ti-13Nb-13Zr in protein solutions, Biomaterials 20 (1999) 631-637

[11] A. T. Kuhn, Corrosion of Co-Cr alloys in aqueous environments, Biomaterials 2 (1981) 68-77

[12] R. Liu, M.Yao, X. Wu, Influence of carbon content in cobalt-based superalloys on mechanical and wear properties, Transactions of the ASME 126 (2004) 204-212

[13] D. Dowson, C. Hardaker, M. Flett, H.G. Isaac, A hip joint simulator study of the performance of metal-on-metal joint Part II: Design, Arthroplasty 19 (2004) 118-123

[14] J.B. Medley, Comparison of alloys and designs in a simulator study of metal on metal implants, Clinical Orthopaedics and Related Research 329S (1996) 148-159

[15] G.C. Clark, D.F. Williams, The effects of proteins on metallic corrosion, Biomedical Materials 16 (1982) 125-134

[16] A. Kocijan, I. Milosev, The influence of complexing agent and proteins on the corrosion of stainless steels and their metal components, Materials Science 14 (2003) 69-77

[17] R.L. Williams, The interfacial reaction between implantable materials and proteins, University of Liverpool, 1986

[18] Y. Yan, A. Neville, D. Dowson, Biotribocorrosion - an appraisal of the time dependence of wear and corrosion interactions - Part I: The role of corrosion, Journal of Physics D: applied physics 39 (2006) 3200-3205

[19] Y. Yan, A. Neville, D. Dowson, Biotribocorrosion - an appraisal of the time dependence of wear and corrosion interactions - Part II: Surface analysis, Journal of Physics D: applied physics 39 (2006) 3206-3212

[20] Y. Yan, A. Neville, D. Dowson, Understanding the role of corrosion in the degradation of metal-on-metal implants, Proc Instn Mech Engrs Part H: Journal of Engineering in Medicine 220 (2006)

173-180

[21] Y. Yan, A. Neville, D. Dowson, S. Williams, Tribocorrosion in implants - assessing high carbon and low carbon Co-Cr-Mo alloys by in-situ electrochemical measurements, Tribology International 39 (2006) 1509-1507

[22] S. Mischler, S. Debaud, D. Landolt, Wear-accelerated corrosion of passive metals in tribocorrosion systems, Electrochemical Society 145 (1998) 750-758

[23] T. Hanawa, M. Ota, Calcium Phosphate naturally formed on titanium in electrolyte solution, Biomaterials 12 (1991) 767-774

Figure captions

Figure 1 Schematic representation of tribo-electrochemical cell

Figure 2 E_{corr} versus time for HC CoCrMo in DMEM for 4 hours tests

Figure 3 E_{corr} versus time for LC CoCrMo in DMEM for 4 hours tests

Figure 4 E_{corr} versus time for 316L in DMEM for 4 hours tests

Figure 5 E_{corr} versus time for HC CoCrMo in 0.36% NaCl for 4 hours tests

Figure 6 E_{corr} versus time for LC CoCrMo in 0.36% NaCl for 4 hours tests

Figure 7 E_{corr} VS. time for 316L in 0.36% NaCl for 4 hours tests

Figure 8 Material total volume loss without and with applied CP in three environments.

Figure 9 Co $2p_{3/2}$ peaks obtained from the wear scar for HC CoCrMo in DMEM and 0.36% NaCl

Figure 10 Anodic polarization (AP) curves for HC CoCrMo in (a) DMEM (b) 0.36% NaCl under sliding and in static conditions

Figure 11 Anodic polarization (AP) and friction coefficient under rubbing for (a) 316L (b) LC CoCrMo

in different solutions

Figure 12 2 cycles of sliding for LC CoCrMo in DMEM (a) current and velocity (b) friction force.

Figure 13 Current and friction curves at 0.2 V applied potential for (a) HC CoCrMo (b) LC CoCrMo and (b) 316L in DMEM

Figure 14 Current and friction curves at 0.2 V applied potential for (a) HC CoCrMo (b) LC CoCrMo and (c) 316L in 0.36% NaCl

Table caption

Table 1 Chemical composition and microhardness for all materials

Table

Table 1 Chemical composition and microhardness for all materials

Materials	C	Co	Cr	Mo	Fe	Ni	HV_{500g}
HC CoCrMo	0.19	Bal.	27.3	5.8	0.41	0.7	463±11.4
LC CoCrMo	0.05	Bal.	27.4	5.7	0.17	0.1	448 ±15.6
316L	0.03		17		Bal.	13	291 ±18.1

Figures

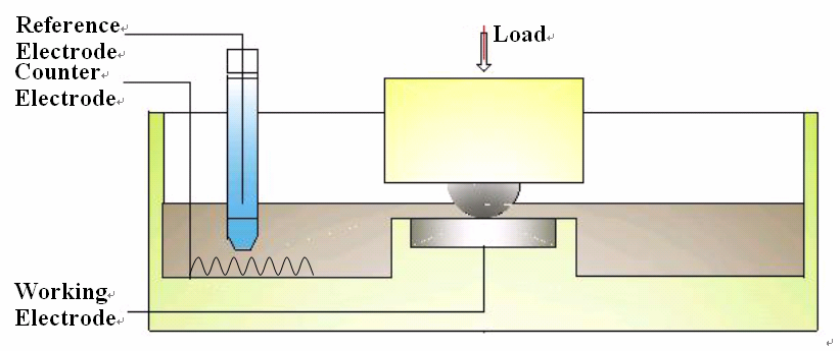

Figure 1 Schematic representation of tribo-electrochemical cell

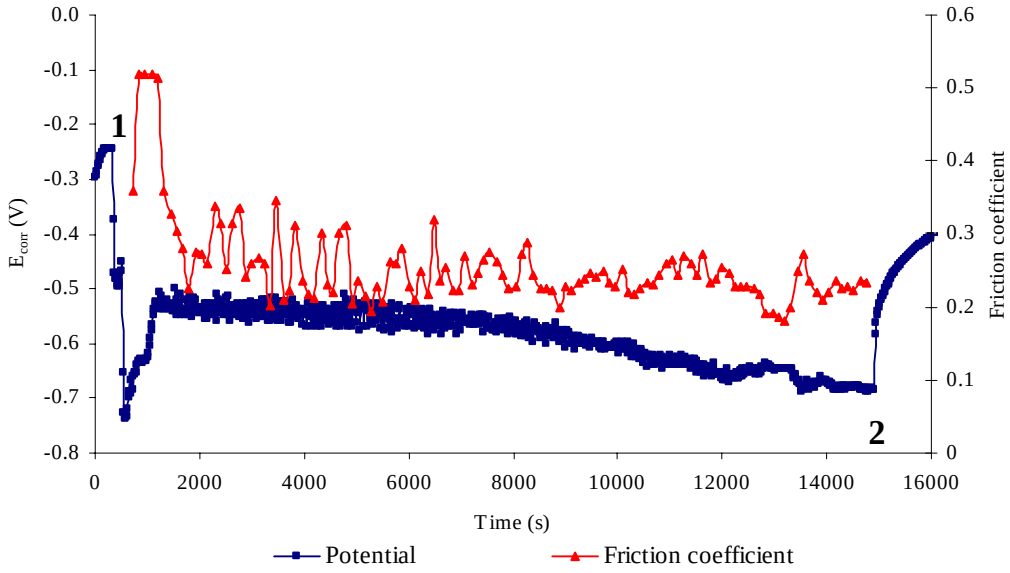

Figure 2 E_{corr} versus time for HC CoCrMo in DMEM for 4 hours tests

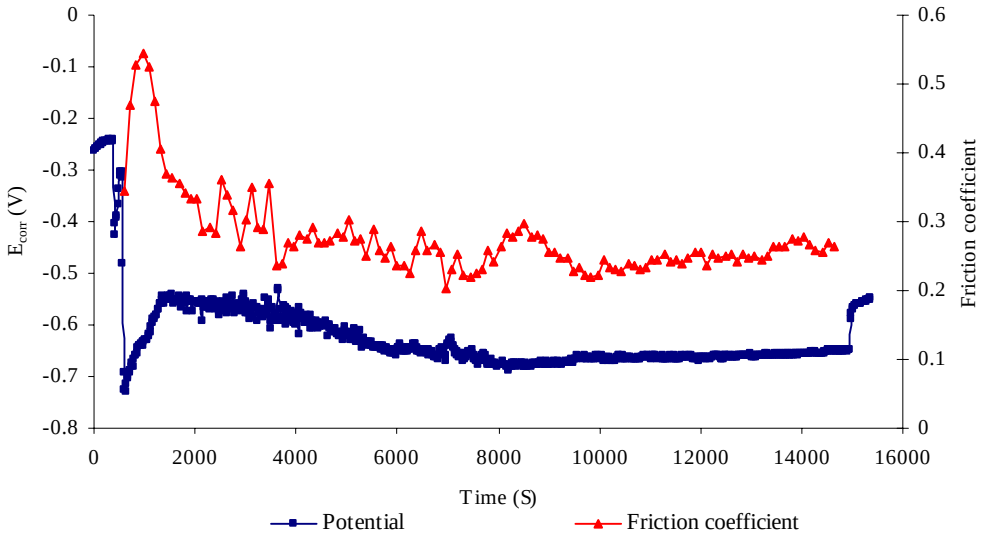

Figure 3 E_{corr} versus time for LC CoCrMo in DMEM for 4 hours tests

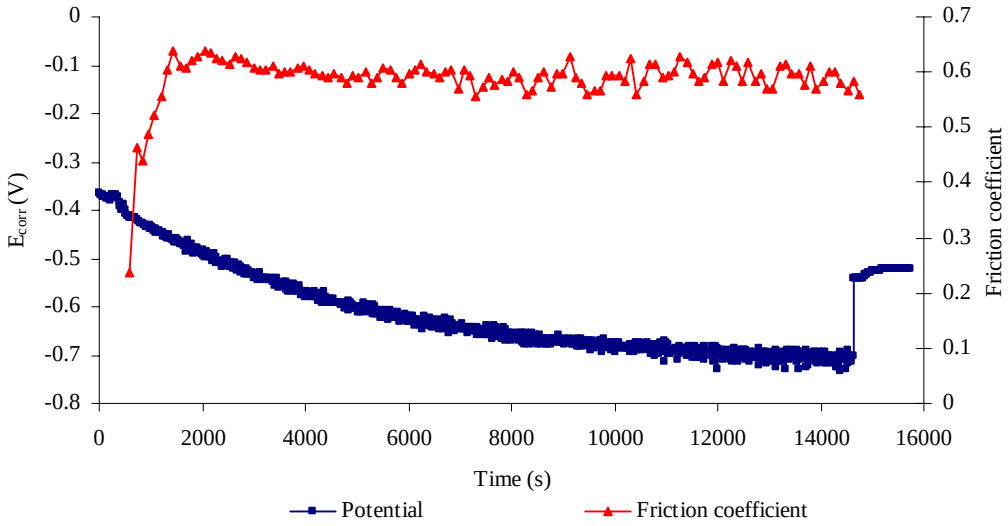

Figure 4 E_{corr} versus time for 316L in DMEM for 4 hours tests

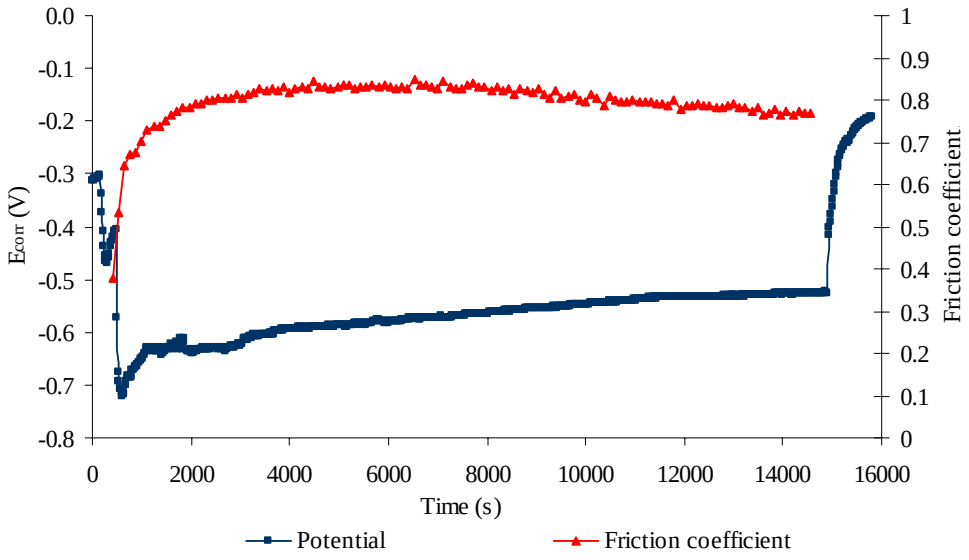

Figure 5 E_{corr} versus time for HC CoCrMo in 0.36% NaCl for 4 hours tests

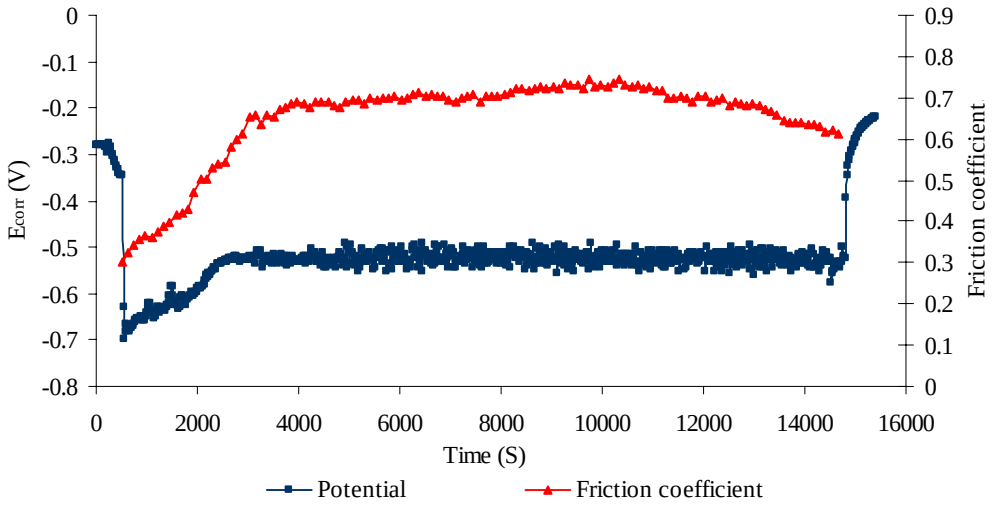

Figure 6 E_{corr} versus time for LC CoCrMo in 0.36% NaCl for 4 hours tests

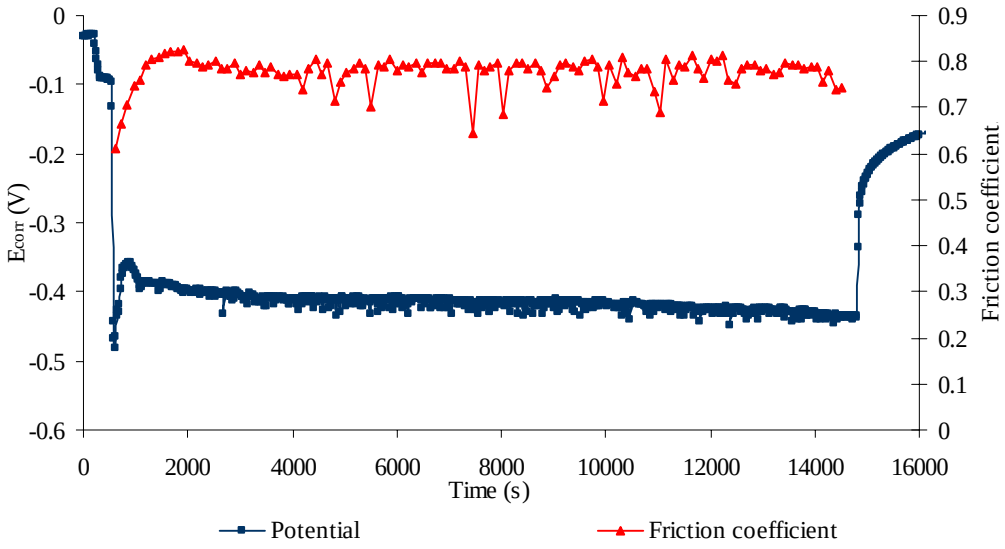

Figure 7 E_{corr} VS. time for 316L in 0.36% NaCl for 4 hours tests

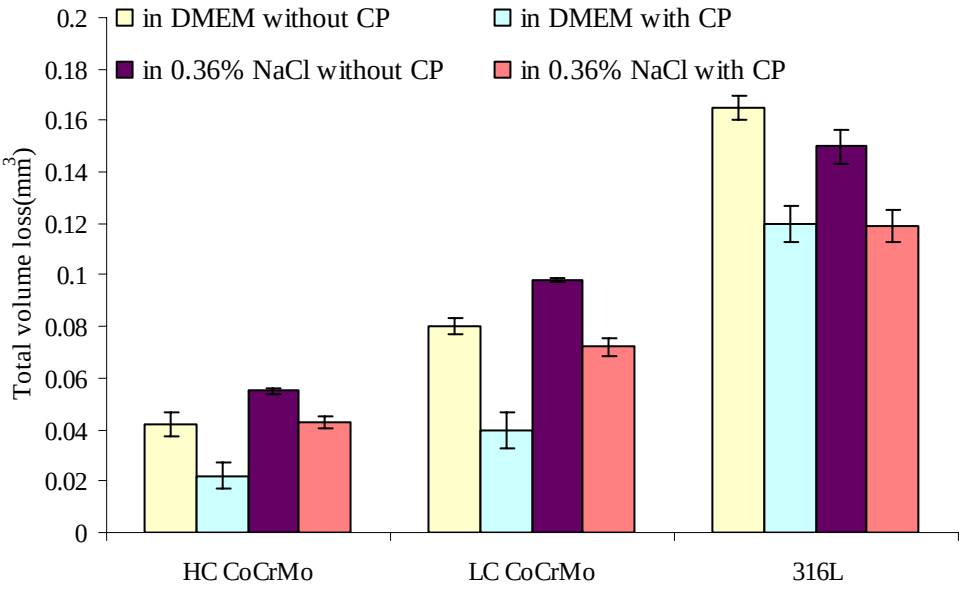

Figure 8 Material total volume loss without and with applied CP in three environments.

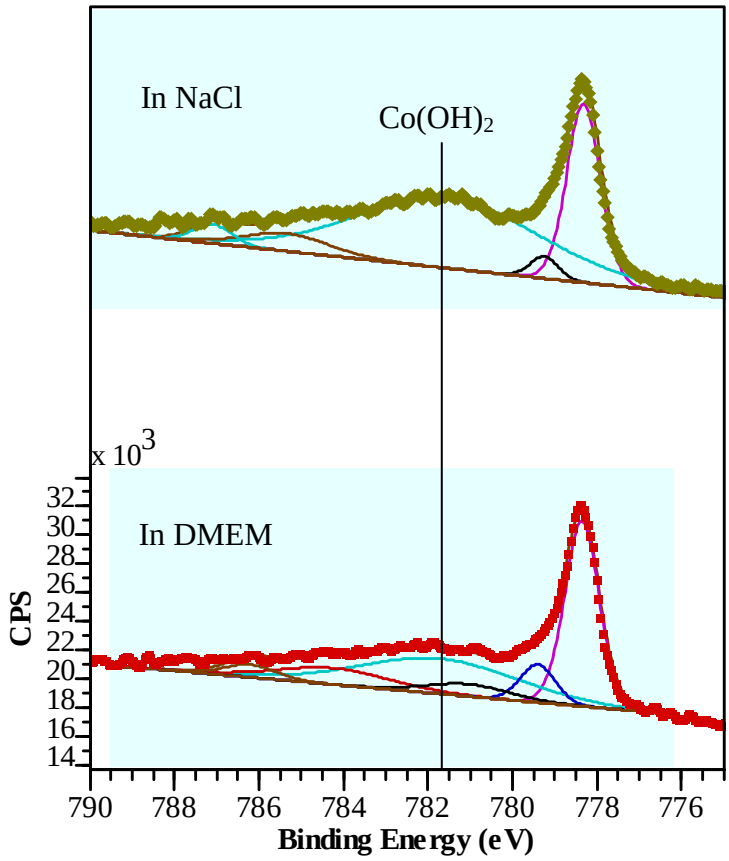

Figure 9 Co $2p_{3/2}$ peaks obtained from the wear scar for HC CoCrMo in DMEM and 0.36% NaCl

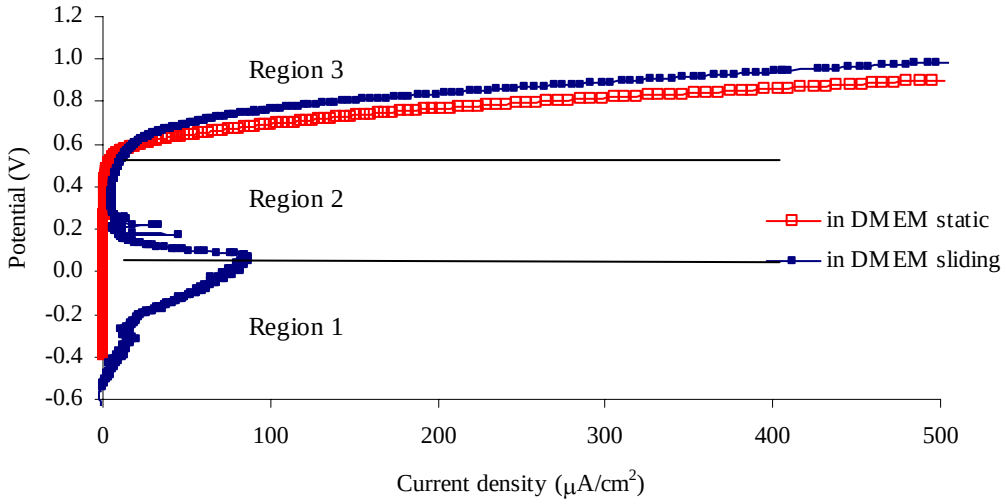

(a)

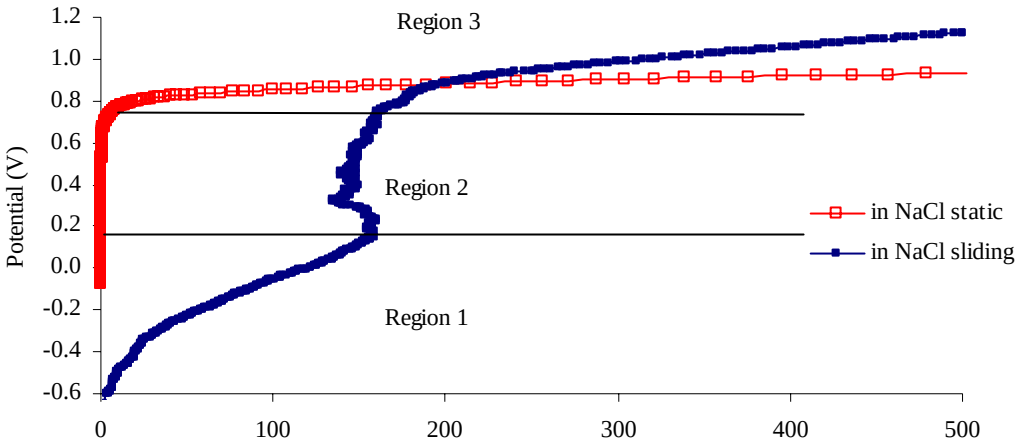

(b)

Figure 10 Anodic polarization (AP) curves for HC CoCrMo in (a) DMEM (b) 0.36% NaCl under sliding and in static conditions

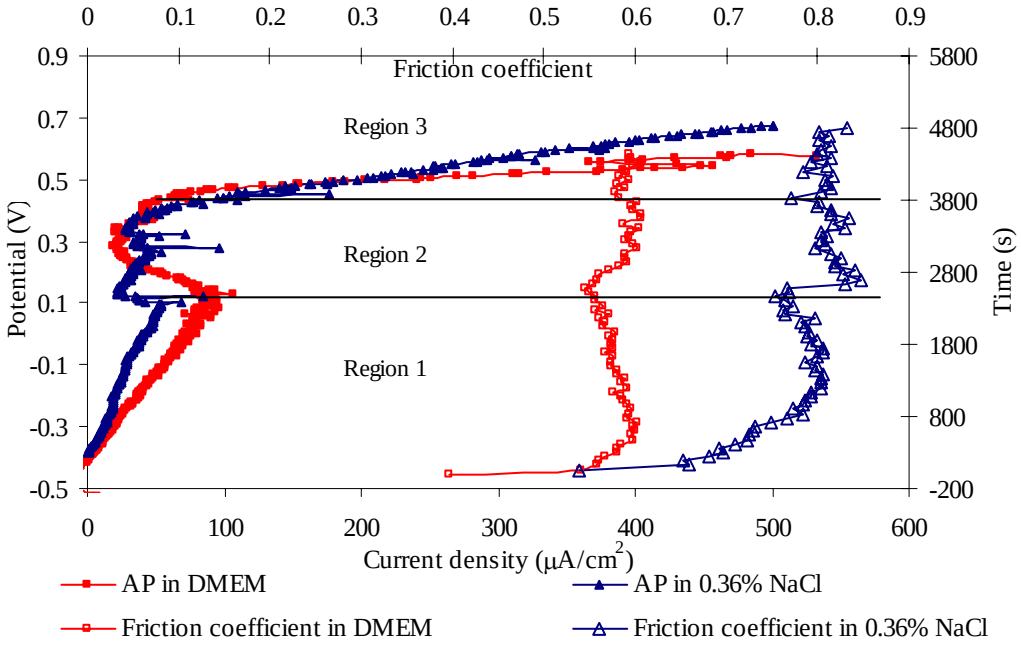

(a)

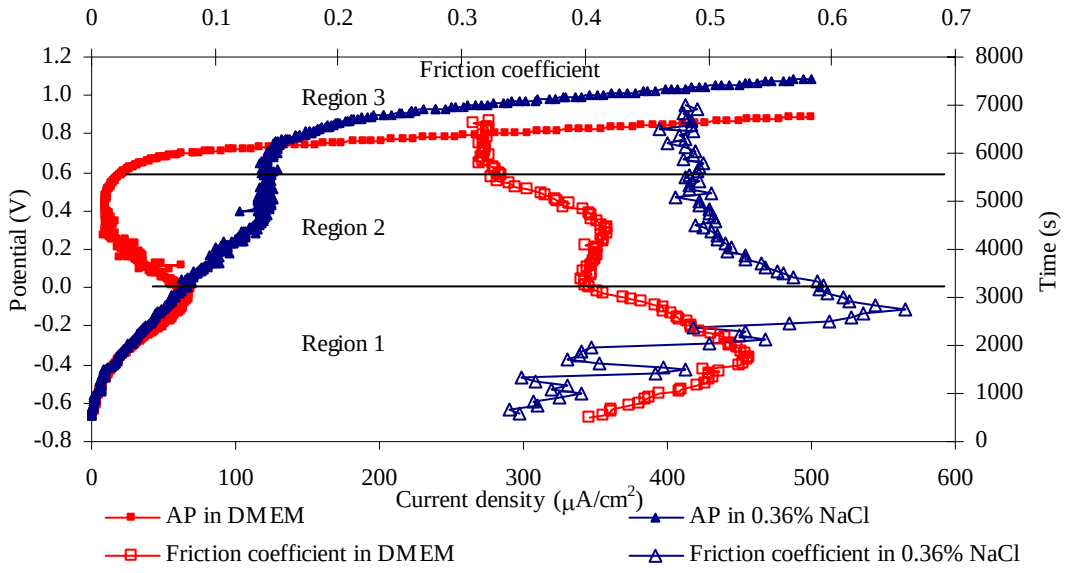

(b)

Figure 11 Anodic polarization (AP) and friction coefficient under rubbing for (a) 316L (b) LC CoCrMo in different solutions

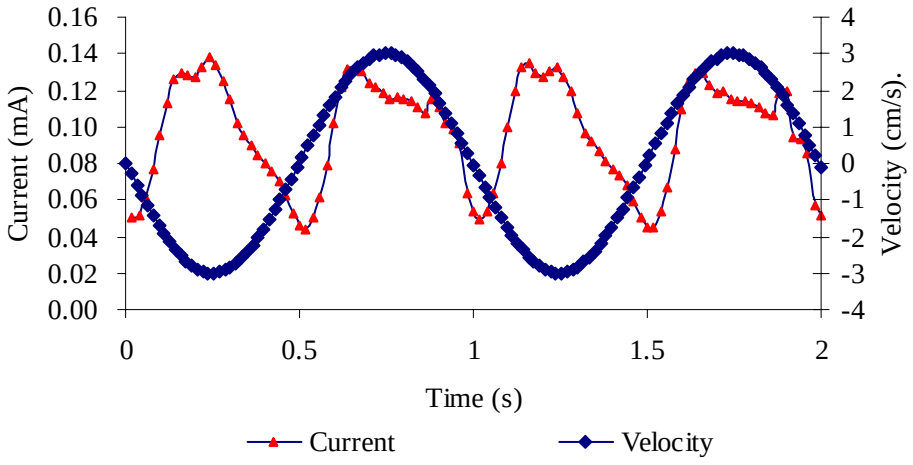

(a)

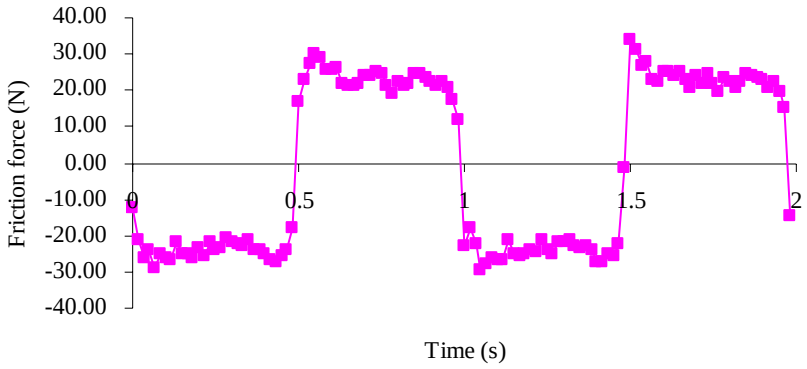

(b)

Figure 12 2 cycles of sliding for LC CoCrMo in DMEM (a) current and velocity (b) friction force.

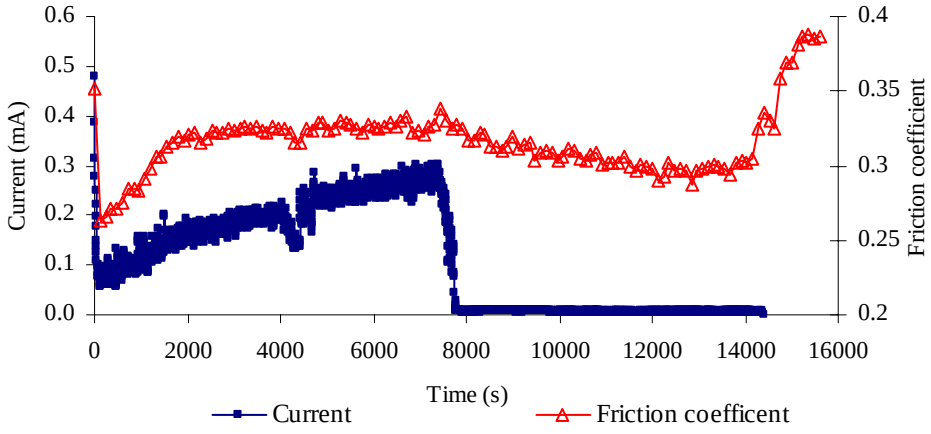

(a)

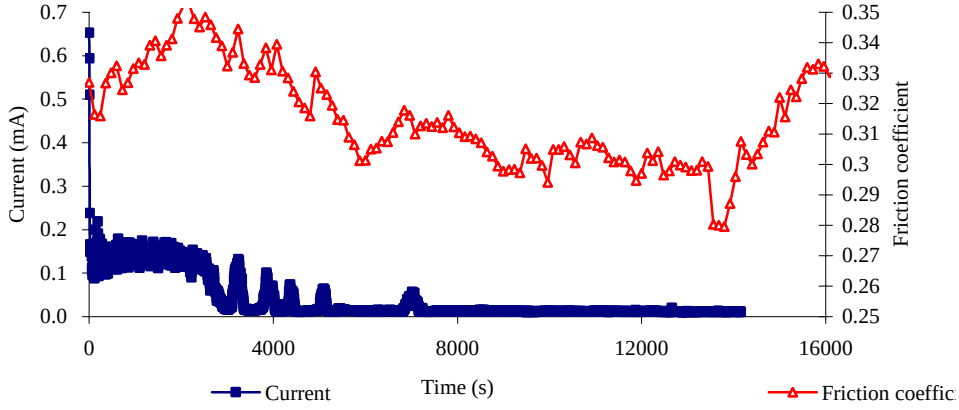

(b)

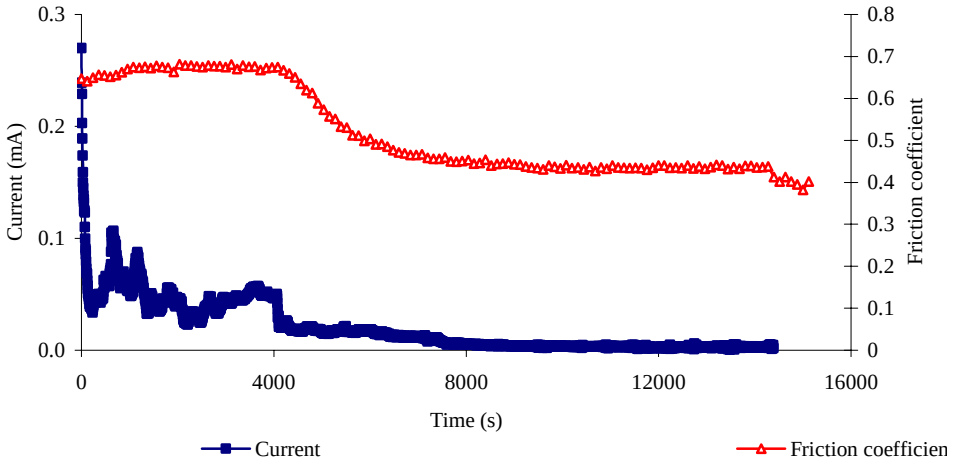

(c)

Figure 13 Current and friction curves at 0.2 V applied potential for (a) HC CoCrMo (b) LC CoCrMo and (b) 316L in DMEM

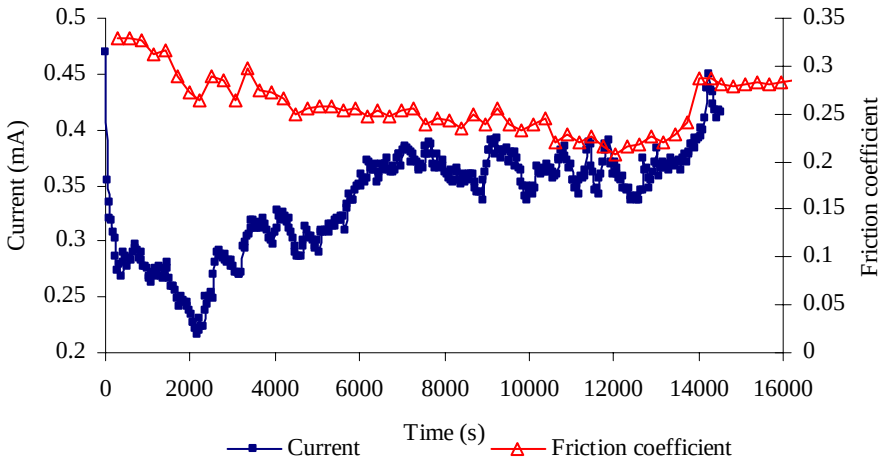

(a)

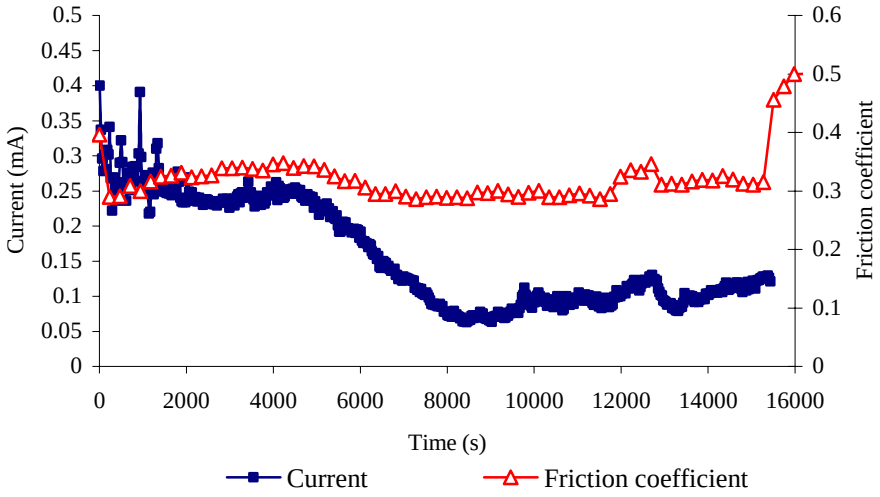

(b)

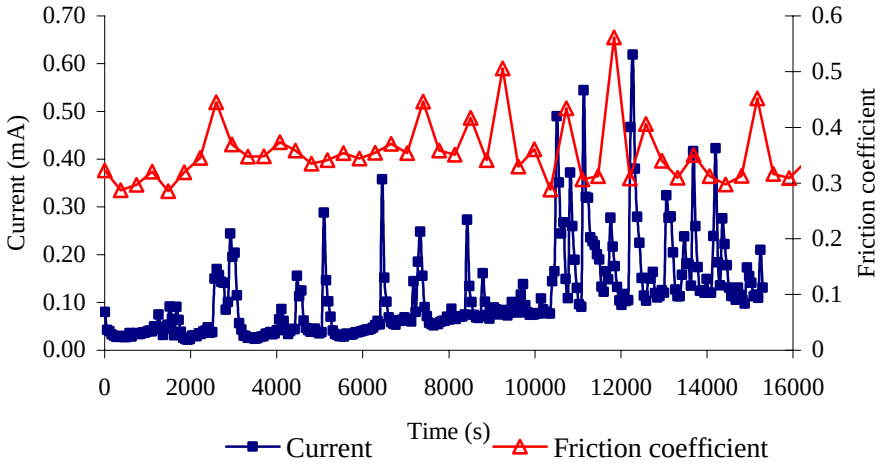

(c)

Figure 14 Current and friction curves at 0.2 V applied potential for (a) HC CoCrMo (b) LC CoCrMo and (c) 316L in 0.36% NaCl